Vibration characterization procedure of piezoelectric ceramic parameters

Application to low-cost thin disks made of piezoceramics

Yann Meyer[a] and Remy Lachat[b]

IRTES-M3M, UTBM, 90010 Belfort Cedex, France

Abstract. To integrate new functionalities inside the mechanical structures for active vibration control, mechatronic, energy harvesting or fatigue management, it is necessary to developp a real fully distributed set of transducers and to include them at the heart of composite materials. To reach this goal, it is absolutely necessary to limit the cost of the numerous transducing elements with respect to the global system cost and, in the same time, to well-know the electromechanical behavior of theses transducers in order to well-design the system controller. In this paper, an experimental non-destructive procedure based on the analysis of anti-resonance and resonance frequencies of the transducers is proposed for determining the material coefficients of interest. This measurement process is applied to low-cost thin disks made of piezoceramics.

1. Introduction

The composite structures with smart transducers included at the heart of the material [1] have a great potential for developing materials with new integrated functionalities as active vibration control, mechatronic, energy harvesting or fatigue management [2]. Active metamaterials with a real fully distributed set of transducers directly integrated can be designed. However, for the development of applications for a large number of consumers, it is necessary to manage the global cost of the device and so the cost of the numerous transducers used to create the distributed network. The use of low-cost transducers implies to correctly and fully characterize each sample selected to custom the controller and to obtain good performances of the final device. The identification processes for a smart composite structure are generally based on a vibration characterization of the whole active composite structure [1,3]. In this article, the choice is different and oriented system engineering. The transducers are characterized before the manufacturing process of the composite structure [4–6]. With the material coefficients obtained and a knowledge of the behavior deviation after the integration process, it is possible to obtain a quite good approximation of the modified material coefficients. At this point, it is possible to develop a numerical model based on these data. The paper is organized as follows. Section 2 describes the numerical models development in order to obtain the useful relationships for determining the material parameters of interest. In the next section, the measurement process with the experimental apparatus is explained. In Sect. 4, experimental results for a set of piezoceramic thin disks are given. Finally, concluding remarks and perspectives of this work are provided.

---

[a] e-mail: yann.meyer@gmail.com
[b] e-mail: remy.lachat@utbm.fr

2. Numerical models development

2.1. Linear theory of piezoelectricity

In linear piezoelectricity, the equations of linear elasticity are coupled to the charge equation of electrostatics by means of the piezoelectric constants. So, the piezoelectric effect is described by one pair of constitutive relations. Four different pairs can describe the same phenomenon. The different coefficients of these relations are related by transfer equations. The choice of the pair used depends on the final modeling. For instance, written in the *e-form* according to the IEEE standard [7,8], the constitutive equations are Eqs. (1) and (2).

$$T_p = c_{pq}^E S_q - e_{kp} E_k \qquad (1)$$

$$D_i = e_{iq} S_q + \varepsilon_{ik}^S E_k \qquad (2)$$

where

$$S_q = S_{ij} \text{ when } i = j, \ p = 1, 2, 3 \qquad (3)$$

$$S_q = 2S_{ij} \text{ when } i \neq j, \ p = 4, 5, 6 \qquad (4)$$

with

$$S_{ij} = \frac{1}{2}(u_{i,j} + u_{j,i}) \qquad (5)$$

T_p, S_q, u_i, D_i, E_k are, respectively, the components of stress, strain, mechanical displacement, electric displacement and electric field. The electric field vector E_k is derivable from an electric potential φ, as shown in Eq. (6).

$$E_k = -\varphi, k \qquad (6)$$

c_{pq}^E, e_{kp} and ε_{ik}^S are respectively the elastic constants at constant electric displacement, piezoelectric coupling coefficients and dielectric constants at constant strain. The piezoelectric material is assumed to be associated

with the crystallographic class 6 mm of the hexagonal crystal system. Consequently, Eqs. (7), (8) and (9) are respectively the arrays of the piezoelectric, elastic and dielectric constant for a ceramic polarization in the thickness direction.

$$e_{kp} = \begin{bmatrix} 0 & 0 & 0 & 0 & e_{15} & 0 \\ 0 & 0 & 0 & e_{15} & 0 & 0 \\ e_{31} & e_{31} & e_{33} & 0 & 0 & 0 \end{bmatrix} \tag{7}$$

$$c_{pq}^E = \begin{bmatrix} c_{11}^E & c_{12}^E & c_{13}^E & 0 & 0 & 0 \\ c_{12}^E & c_{11}^E & c_{13}^E & 0 & 0 & 0 \\ c_{13}^E & c_{13}^E & c_{33}^E & 0 & 0 & 0 \\ 0 & 0 & 0 & c_{44}^E & 0 & 0 \\ 0 & 0 & 0 & 0 & c_{44}^E & 0 \\ 0 & 0 & 0 & 0 & 0 & \frac{1}{2}(c_{11}^E - c_{12}^E) \end{bmatrix} \tag{8}$$

$$\varepsilon_{ik}^S = \begin{bmatrix} \varepsilon_{11}^S & 0 & 0 \\ 0 & \varepsilon_{11}^S & 0 \\ 0 & 0 & \varepsilon_{33}^S \end{bmatrix}. \tag{9}$$

2.2. Equations of motion

In a piezoelectric body Ω_0, the mechanical displacement constants, u_i, and the electric potential, φ, are solutions of the equations of equilibrium and the Gauss's law in electrostatics [9,10].

$$T_{ij,i} + f_j = \rho.\ddot{u}_j \tag{10}$$

$$D_{i,i} = \rho_e = 0 \tag{11}$$

where ρ, ρ_e and f_j are, respectively, the mass density, the volumic electric charge density and the volumic external loads. The piezoelectric body is not infinite. Consequently, Eqs. (10) and (11) are associated to boundary conditions. The mechanical boundary conditions are:

$$\begin{cases} u_i = u_{i0} & \forall x \in \partial\Omega_0^u \\ T_{ij}n_i = \bar{t}_i & \forall x \in \partial\Omega_0^T \end{cases} \tag{12}$$

where $\partial\Omega_0^u$ and $\partial\Omega_0^T$ are respectively the mechanical Dirichlet conditions and the mechanical Neumann conditions. n_i are the components of a vector normal to $\partial\Omega_0^T$. The electric boundary conditions are:

$$\begin{cases} V = 0 & \forall x \in \partial\Omega_0^V \\ V = V_a & \forall x \in \partial\Omega_a^V \\ D_i.m_i = 0 & \forall x \in \partial\Omega_0^q \end{cases} \tag{13}$$

where $\partial\Omega_0^V$, $\partial\Omega_a^V$ and $\partial\Omega_0^q$ are respectively the electric Dirichlet conditions, the electric Dirichlet conditions associated to the electroded faces (the input and output surfaces of the system) and the electric Neumann conditions. m_i are the components of a vector normal to $\partial\Omega_0^q$.
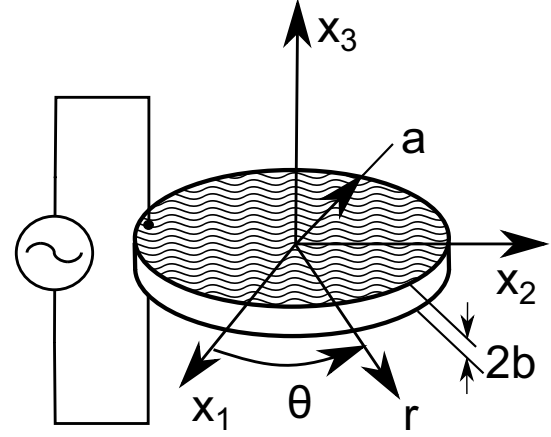

Figure 1. Electroded thin disk in cartesian and cylindrical coordinate systems.

2.3. Modeling assumptions

The structure studied is a disk made of a piezoelectric ceramic and polarized in the thickness direction. The diameter to thickness ratio is strongly large (typically, >50) so that the boundary conditions can be ignored and the natural modes are considered perfectly uncoupled [8,11]. The major faces of the disk are completely coated with electrodes. The minor surface is unelectroded. A Cartesian and cylindrical coordinate systems are used and shown in Fig. 1. The top and bottom faces of the disk are located at $x_3 = \pm b$. The radius of the disk is a.

According to the above remarks, the assumptions (14), (15), (16), (17) and (18) are formulated. The electric potential is assumed linear.

$$E_1 = E_2 = 0 \tag{14}$$

$$T_4 = T_5 = 0 \tag{15}$$

$$c_{13}^E = 0 \tag{16}$$

$$c_{44}^E = 0 \tag{17}$$

$$k_t = k_{33}. \tag{18}$$

2.4. Radial and thickness modes vibration in thin disks

So as to obtain the equations of motion, the constitutive equations of piezoelectricity are written in the cylindrical coordinate system. So, the variables are the radius r, the angle θ and the dimension along the thickness-axis, z. For this natural mode, some additional assumptions can be formulated. The radial motion implies $u_\theta = 0$. The pair of constitutive relations (1) and (2) becomes the set of equations from (19) to (22).

$$T_{rr} = c_{11}^E u_{r,r} + c_{12}^E \frac{u_r}{r} - e_{31}E_3 \tag{19}$$

$$T_{\theta\theta} = c_{11}^E \frac{u_r}{r} + c_{12}^E u_{r,r} - e_{31} E_3 \qquad (20)$$

$$T_3 = c_{33}^E \frac{u_z}{z} - e_{33} E_3 \qquad (21)$$

$$D_3 = e_{31}\left(u_{r,r} + \frac{u_r}{r}\right) + e_{33} u_{z,z} + \varepsilon_{33}^S E_3. \qquad (22)$$

The mechanical equations of motion expressed in cylindrical coordinates are Eqs. (23) and (24). The Gauss's law gives Eq. (25).

$$\frac{\partial T_{rr}}{\partial r} + \frac{T_{rr} - T_{\theta\theta}}{r} = \rho \ddot{u}_r \qquad (23)$$

$$\frac{\partial T_3}{\partial z} = \rho \ddot{u}_z \qquad (24)$$

$$\frac{\partial D_3}{\partial z} = 0. \qquad (25)$$

The mechanical and electric boundary conditions are given by the set of Eq. (26).

$$\begin{cases} T_{rr} = 0 & \text{at } r = a \\ T_3 = 0 & \text{at } x_3 = \pm b \\ \varphi = \pm \frac{V}{2} e^{j\omega t} & \text{at } x_3 = \pm b. \end{cases} \qquad (26)$$

Substituting from (19), (20), (19) and (22) for the stress components and the electric displacement and using the assumptions formulated, equations from (27) to (29) are obtained.

$$c_{11}^E\left(u_{r,rr} + \frac{u_{r,r}}{r} - \frac{u_r}{r^2}\right) = \rho \omega^2 u_r \qquad (27)$$

$$c_{33}^E u_{z,zz} = \rho \omega^2 u_z \qquad (28)$$

$$e_{31}\left(u_{r,rz} + \frac{u_{r,z}}{r}\right) + e_{33} u_{z,zz} = 0. \qquad (29)$$

2.5. Relationships used for determining the parameters of interest

By solving the equations of motion and by integrating electric displacement over the electroded surfaces, the electrical impedance of the disk is obtained. From this electrical impedance expression, the relationships necessary to compute the parameters of interest are obtained [4–6]. These relationships are based on the system behavior at the resonance and anti-resonance frequencies for radial mode vibration, f_{rp} and f_{ap} respectively, and thickness mode vibration, f_{r3} and f_{a3} respectively. For determining the parameters of interest from the radial mode, the first overtone resonant frequency, $f_{rp}^{(2)}$, is also necessary [6]. The frequency detection is based on the zero phase angle method to avoid the errors due to the damping effect.

$$\varepsilon_{33}^T = \varepsilon_{3r}\varepsilon_0 = C^T \frac{2b}{\pi a^2} \qquad (30)$$

$$\varepsilon_{33}^S = C^S \frac{2b}{\pi a^2} \qquad (31)$$

$$k_t^2 = \frac{\pi}{2}\frac{f_{r3}}{f_{a3}} cotan\left(\frac{\pi}{2}\frac{f_{r3}}{f_{a3}}\right) \qquad (32)$$

$$\varepsilon_{33}^S = \varepsilon_{33}^T[(1 - k_t^2)(1 - k_p^2)] \qquad (33)$$

$$C_{33}^E = 4\rho f_{a3}^2 (2b)^2 (1 - k_{33}^2) \qquad (34)$$

$$e_{33} = k_t(\varepsilon_{33}^S 4\rho f_{a3}^2 (2b)^2)^{1/2} \qquad (35)$$

$$\eta \frac{J_0(\eta)}{J_1(\eta)} = 1 - \sigma_p \qquad (36)$$

$$k_{31}^2 = k_p^2 \frac{1 - \sigma_p}{2} \qquad (37)$$

$$C_{11}^E = \rho\left(\frac{2\pi f_{rp} a}{\eta}\right)^2 \qquad (38)$$

$$C_{12}^E = \sigma_p C_{11}^E \qquad (39)$$

$$e_{31} = k_{31}\left(\frac{\varepsilon_{33}^T C_{11}^E (C_{11}^E - C_{12}^E)}{(C_{11}^E + C_{12}^E)}\right)^{1/2} \qquad (40)$$

where ε_{33}^T, ε_{3r} ε_0, C^T, C^S, k_t, k_p, η, $J_0(x)$, $J_1(x)$, σ_p are, respectively, the dielectric constant at constant stress along the z-axis, the relative dielectric constant, the dielectric constant of the free space, the free electric capacitance, the electromechanical coupling factor along the thickness-axis, the planar electromechanical coupling factor, the root of Eq. (36), the Bessel function of first kind and zero order, the Bessel function of first kind and first order and the planar Poisson's ratio.

3. Measurement process

3.1. Experimental setup

The experimental data from electric impedance measurements of piezoelectric thin disks are obtained with an Agilent E 5100A network analyser, located in the FEMTO ST Institute. An in-house device is used to obtain the electric contacts with the samples. The experimental setup with a sample to be measured is depicted in Fig. 2. In Fig. 3, a typical impedance profiles (magnitude and phase) for radial mode vibration is given between 1 kHz and 1 MHz. An Unigor 380 multimeter is also used to measure the electric capacitance of the thin disk at low frequency.
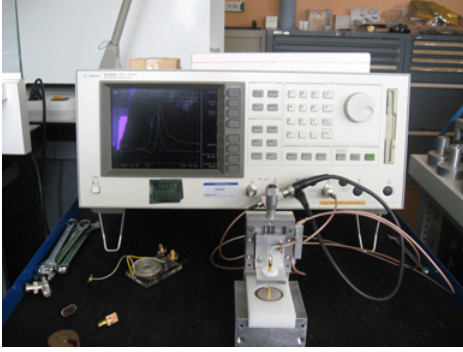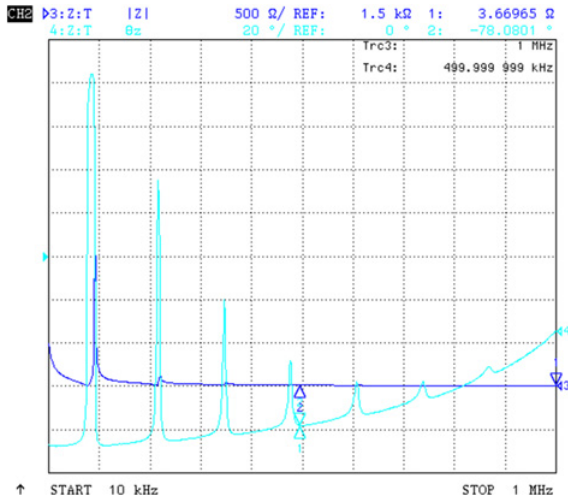
Figure 2. Experimental setup.

Figure 3. Typical impedance profiles (magnitude and phase) for radial mode vibration between 1 kHz and 1 MHz.

3.2. Experimental procedure for determining the parameters of interest

For determining the parameters of interest, three sets of measurements are performed as shown in Fig. 4.

For the first step, the dimensions (diameter and thickness) of each thin disk and the electric capacitances, at low frequency (65 Hz) and at high frequency (1 MHz), are measured. These frequencies are selected to be far away from resonance phenomenons and to be the upper and lower bounds of the studied resonance phenomenons (here, the radial mode vibration). By using Eqs. (30) and (31), ε_{33}^T and ε_{33}^S are calculated.

For the second step, the fundamental resonance and anti-resonance frequencies for the thickness-mode vibrations are measured. The typical values are 12.536 MHz for the fundamental resonance frequency and 12.675 MHz for the fundamental anti-resonance frequency. Equation (32) gives the thickness coupling coefficient k_t. With k_t, ε_{33}^T, ε_{33}^S and Eq. (33), the planar coupling coefficient k_p is calculated. C_{33}^E and e_{33} are computed with Eqs. (34) and (35).

For the third and last step, Eq. (36) is exploited to obtained σ_p and η thanks to Table 1. This procedure is clearly and completely described in [6]. To summarize the process, the ratio $\frac{f_{rp}^{(2)}}{f_{rp}}$ (typically, 2.6) is computed
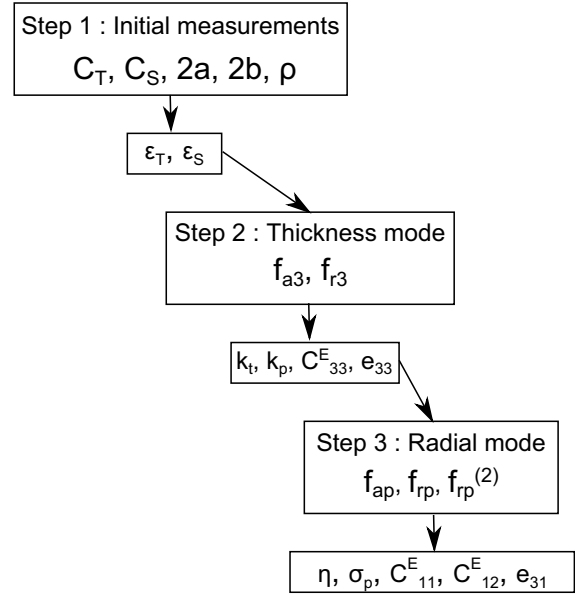

Figure 4. Experimental procedure for determining the parameters of interest.

Table 1. Relation between σ_p and $\frac{f_{rp}^{(2)}}{f_{rp}}$ from Eq. (36).

$\dfrac{f_{rp}^{(2)}}{f_{rp}}$	σ_p	η
2.6304	0.3	2.0489
2.6234	0.31	2.0551
2.6165	0.32	2.0612
2.6095	0.33	2.0674
2.6029	0.34	2.0735
2.5962	0.35	2.0795
2.5897	0.36	2.0855
2.5832	0.37	2.0915
2.5768	0.38	2.0974
2.5735	0.39	2.1033
2.5642	0.4	2.1092

and used to find the value of σ_p and η in Table 1 for each piezoceramic sample. Let's note that, for radial mode vibration, the typical values are 84.81 kHz for the fundamental resonance frequency, 100.17 kHz for the fundamental anti-resonance frequency and 220.5 kHz for the first overtone resonance frequency. Thus, the missing parameters of interest are calculated with equations from (37) to (40).

4. Experimental results

For this study, 40 low-cost piezoceramic samples are measured and analyzed. The diameter to thickness ratio is strongly large (approximatively, >180). Consequently, the different assumptions expressed are available. The material coefficients of these samples are calculated according to the experimental procedure presented in Sect. 3.2.

In Table 2, only the average material coefficients and their standard deviation are given. Let the reader note that the mass density, ρ, is measured according to [11] (the minimum quantity doesn't permit to compute a standard

Table 2. Parameters of interest from the measured data.

Parameter of interest	Unit	Nominal value	Standard deviation (%)
$2a$	mm	24.7	0
ρ	$Kg.m^{-3}$	7227	0
$2b$	μm	135	5
ε_{33}^T	$F.m^{-1}$	1894	3.9
ε_{33}^S	$F.m^{-1}$	1195	6
k_t	-	0.17	6.2
k_{31}	-	0.34	4.6
k_p	-	0.59	4.9
e_{33}	$C.m^{-2}$	5.00	6.5
e_{31}	$C.m^{-2}$	19.95	6
C_{11}^E	$N.m^{-1}$	$1.011e^{11}$	1.4
C_{12}^E	$N.m^{-1}$	$3.506e^{10}$	2.7
C_{33}^E	$N.m^{-1}$	$8.195e^{10}$	5.2
σ_p	-	0.345	2.8

deviation) and the disk diameter has a very small deviation probably due to the manufacturing process used. The measurements are completed by a mechanical quality factor measurement for the radial mode vibrations with the 3-dB method [11,12]. The average mechanical quality is 49.4 with a standard deviation of 18.2%. Of course, the material coefficients and the mechanical quality factor are also available for each sample. The standard deviation values show a quite good manufacturing homogeneity despite of a low cost. Let the reader remark a quite low planar coupling coefficient, k_p and, globally, the coupling and piezoelectric coefficients are quite limited. This fact has to be managed by the strategy used for modifying the structure behavior, for instance, in an active vibration control process.

5. Concluding remarks and perspectives

This paper has detailed analytical relationships for determining the material coefficients of interest for low-cost piezoceramic thin disks and the measurement process in order to obtain the input data. This measurement process has been applied to 40 low-cost thin disks made of piezoceramics.

The next step of this work is to wrap the 40 piezoceramic disks with a carbon-fiber composite structure. The idea is to evaluate the piezoelectric behavior deviation after the manufacturing process for each sample. For this characterization, the measurement procedure developped in this paper will be used.

References

[1] S. Chesne, C. Jean-Mistral, L. Gaudiller, Smart Mater. Struct. **22**, 075007 (2013)

[2] G. Meyer, J. Valldorf, W. Gessner, *Advanced Microsystems for Automotive Applications 2009* (Springer, 2009)

[3] P. Berik, A. Benjeddou, M. Krommer, Smart Mater. Struct.l **13**, 567 (2014)

[4] J. Fialka, P. Benes, *Measurement of Piezoelectric Ceramic Parameters*, in *13th International Carpathian Control Conference (ICCC)* (2012), Vol. 1

[5] M. Brissaud, IEEE Trans. ultrasonics, ferroelectrics and frequency control **38**, 603 (1991)

[6] A.H. Meitzler, H.M. O'Bryan, H.F. Tiersten, IEEE Trans. Sonics Ultrason. **SU-20**, 233 (1973)

[7] I.E.E.E. Standard ANSI/IEEE Std 176-1987, *IEEE Standard on Piezoelectricity* (The Institute of Electrical and Electronic Engineers Inc., New York, 1987)

[8] I.E.E.E. Standard ANSI/IEEE Std 177-1966, *Standard definitions and methods of measurement for piezoelectric vibrators* (The Institute of Electrical and Electronic Engineers Inc., New York, 1966)

[9] M. Naillon, R. Coursant, F. Besnier, Acta electronica **25**, 341 (1983)

[10] Y. Meyer, M. Collet, Mécanique & Industries **10**, 109 (2009)

[11] E.N. 50324-2 European standard, *Piezoelectric properties of ceramic materials and components, Part 2: Methods of measurement Low power* (CENELEC European Committee for Electrotechnical Standardization, 2002)

[12] A.D. Nashif, D.I.G. Jones, J.P. Henderson, *Vibration damping* (John Wiley, New York, 1985)